AMERICAN SCIENTIFIC PUBLISHERS

Science of Advanced Materials
Vol. 9, pp. 1–10, 2017
www.aspbs.com/sam

ARTICLE

Waterborne Polyurethane/Graphene Oxide Nanocomposites with Enhanced Properties

Haixiang Song[1,2,3,*], Meng Wang[1,2], Yanfei Wang[1], Yadong Zhang[2,*], Ahmad Umar[4,*], and Zhanhu Guo[3,*]

[1]*Department of Chemical and Environmental Engineering, Anyang Institute of Technology, Anyang 455000, China*
[2]*School of Chemical Engineering and Energy, Zhengzhou University, Zhengzhou 450001, China*
[3]*Integrated Composites Laboratory (ICL), Department of Chemical and Biomolecular Engineering, University of Tennessee, Knoxville, Tennessee 37966, USA*
[4]*Department of Chemistry, Faculty of Science and Arts and Promising Centre for Sensors and Electronic Devices (PCSED), Najran University, P.O. Box: 1988, Najran 11001, Kingdom of Saudi Arabia*

ABSTRACT

In this study, one waterborne polyurethane (WPU) pre-polymer was synthesized by using polypropylene glycol (PPG-2000), 2,2-dimethylolpropionic acid (DMPA) and isophorone di-isocyanate (IPDI) via a step-wise reaction. Then, a series WPU/graphene oxide (GO) nanocomposites were prepared by ultra-sonication of GO dispersion and high shear emulsification. The GO and the WPU/GO nanocomposites were characterized by the Fourier transform infrared spectroscopy (FTIR), particle size analysis, X-ray diffraction (XRD), scanning electron microscopy (SEM), transmission electron microscopy (TEM), water contact angles test, atomic force microscopy (AFM), Raman spectroscopy, tensile properties test, thermo-gravimetric analysis (TGA) and differential scanning calorimetry (DSC). The results showed that the WPU/GO emulsions exhibited optimal dispersion stability, the particle size of WPU/GO increased compared with that of virgin WPU. While the GO amount in the WPU/GO nanocomposites was 0.25–0.50 wt% (based on the weight of WPU resin), the GO could be dispersed homogenously, yet the water contact angle values for the WPU/GO films were higher than that of pure WPU, an increase from 58.83° for pure WPU to 61.38° for the GO content of 0.25%, and 62.32° for the GO content of 0.50%, respectively, showing an improvement in the hydrophobic properties. Furthermore, with the GO content increased from 0.00 (WPU0) to 0.25% (WPU1), the tensile strength of the film got 60.69% improvement from 2.90 to 4.66 MPa, whereas the GO content increased from 0.25 (WPU1) to 0.50% (WPU2), the tensile strength of the films decreased from 4.66 to 4.31 MPa, with further increasing GO content, the elongation at break of the WPU/GO films decreased correspondingly. Finally, a better synergy interactions between WPU and GO were observed, and the micro-phase separation was reduced.

KEYWORDS: Nanocomposites, Polyurehtane, Graphene Oxide, Mechanical Properties.

1. INTRODUCTION

Waterborne polyurethane (WPU) has drawn increasing attention recently due to their excellent properties such as high abrasion resistance, large flexibility and strong adhesion to a wide range of substrates. In addition, WPU dispersions are environmental-friendly in comparison with solvent-borne PUs which have been widely used for decades.[1] As an important alternative, WPUs have also been widely used in many industrial applications, such as coatings, adhesives, inks, and so on.[2–5] However, traditional WPUs have some disadvantages such as poor water resistance and mechanical properties that limit their applications. It is desired to modify WPU to provide improved properties such as mechanical strength, hardness, scratch resistance and so on. Among several reported approaches, the application of nanoparticles is one of the most widely used method to improve the properties of WPUs. Proper dispersion of nanoparticles, without aggregation in the WPU, is a fundamental requirement. At present, nanomaterials used for modified-WPU include titania,[6,7] silica,[8,9] Fe_3O_4,[10,11] and graphene[12] etc.

Graphene, one-atom-thick two-dimensional layers of sp^2-bonded carbon network, has attracted a great deal of attention from researchers because of its large surface area, unique electronic, mechanical, and thermal properties.[13,14] Graphite oxide is a layered material

*Authors to whom correspondence should be addressed.
Emails: sxlong2009@qq.com, 13837213690@163.com, ahmadumar786@gmail.com, zguo10@utk.edu
Received: 17 February 2017
Accepted: 28 March 2017

consisting of hydrophilic oxygenated graphene sheets (graphene oxide sheets) bearing oxygen functional groups on their basal planes and edges.[15] The presence of functional groups such as hydroxyl and epoxide functional groups as well as carbonyl and carboxyl groups allows graphite oxide to swell and disperse in water.[16, 17] The synthesis methods and characterizations of graphene have been reviewed in several recent review literatures.[18, 19] Pokharel et al.[20] reported that graphene oxide (GO) dispersion in polyol was prepared and used for the preparation of PU nanocomposites by *in-situ* bulk polymerization. The composites showed a Young's modulus increase of 280.5% through the incorporation of 3 wt% GO. Additionally, an improvement of 40.5% in the tensile strength and 19% in the elasticity were achieved at 1 wt% GO loading. Zhuo et al.[21] prepared WPU/CNT/GO nanocomposites. Their results suggested that modified CNT and GO had been successfully introduced to the PU molecular chains. When the ratio of CNT and GO was 1:2, the thermal decomposition temperature of the composite films was increased by 30 °C than that of pure WPU film. At the same time, water resistance and mechanical properties of the composite films were improved.

In this paper, one waterborne polyurethane (WPU) pre-polymer was synthesized via a step-wise reaction, then a series of WPU/GO nanocomposites were prepared by mixing GO dispersion with the WPU pre-polymer solution and treated with high shear emulsification. In this way, a well dispersed GO WPU nanocomposite was fabricated. Furthermore, the interactions between WPU and GO were observed. The effects of GO nanosheets loadings on the thermal and mechanical properties, and hydrophobicity of the WPU/GO nanocomposites were investigated.

2. EXPERIMENTAL DETAILS

2.1. Materials

Graphite powder (98.0%) was purchased from Damao Co. (Tianjin, China). Isophorone diisocyanate (IPDI) was purchased from Bayer. Polypropylene glycol (PPG-2000) was purchased from Jiangsu Haian Petrochemical Plant, China. 2,2-Dimethylolpropionic acid (DMPA) was supplied by Aladdin. Dibutyltindilautrate (DBTDL) was supplied by Xiya Company (Chengdu, China). Methyl ethyl ketone (MEK) was purchased from Chenqi Co. (Tianjin, China). Triethylamine (TEA), sulfuric acid (98%), sodium nitrate, potassium permanganate, hydrogen peroxide (30%), and hydrochloric acid were analytical grade. The above chemical reagents were used as received without any further treatment.

2.2. Preparation of GO

Graphite oxide was synthesized following a modified Hummers method.[22–25] Briefly, 3 g flake graphite and 1.5 g $NaNO_3$ were placed in a flask. To this mixture, 70 mL H_2SO_4 was added and stirred in an ice water bath for 15 min. Then, 12 g $KMnO_4$ was gradually added over about 30 min and stirred for 30 min. The mixture was allowed to stir for 2 h at 35–45 °C. Then, 150 mL deionized water was added into the mixture slowly and stirred for 15 min at 95 °C. Subsequently, 30 mL 30 wt% H_2O_2 aqueous solution was added and stirred for 30 min at room temperature. The viscous solution turned from blackish purple to brownish yellow and was centrifuged and washed with 5 wt% HCl to remove metal ions. In addition, the mixture was filtered and washed with water until no Cl^- ion was detected. Finally, the sample of graphite oxide was obtained after freeze drying.

To prepare graphene oxide (GO), 1 g graphite oxide was dispersed in 200 mL water to create a yellow–brown dispersion, and the exfoliation of graphite oxide to GO was achieved by ultrasonication for 2 h. After centrifugal separation at 3000 rpm for 5 min, the upper suspension was separated and dried under vacuum at 60 °C to obtain GO.

2.3. Preparation of WPU/GO Nanocomposites

72.19 g PPG-2000 was charged into a four-necked flask and was heated to 80 °C under the protection of N_2 and stirring. A few drops of DBTDL (5 wt% DBTDL based on the MEK) were added into the mixture. Subsequently, 32.87 g IPDI was added into the reactor via addition funnel in 0.5 h. The reaction was maintained for 3.0 h. 32.19 g MEK was added into the flask, followed by addition of 6.76 g DMPA and stirred for an additional 3.0 h at 80 °C. The WPU pre-polymer was obtained.

In a typical experiment for the composite preparation, 0.1 g GO was dispersed in 150 mL distilled water by ultrasonication for 1 h to obtain the GO dispersion. 40 g WPU pre-polymer was added to the dispersion, followed by adding 2.1 g TEA drop-wise to neutralize the DMPA unit of the WPU pre-polymer. The mixture was mixed for 0.5 h under vigorous stirring (1000 rpm) at room temperature, then treated with the high shear emulsification method (12000 rpm) for 3–5 min. The MEK was removed using rotary evaporation under vacuum (0.08 MPa) at 60 °C for 1.0 h. The final solid concentration of the WPU/GO was about 30%. Using this approach, the WPU/GO nanocomposites containing 0.00, 0.25, 0.50, 0.75, 1.00 and 1.25 wt% GO based on the weight of WPU resin were prepared and labeled as WPU0, WPU1, WPU2, WPU3, WPU4, and WPU5, respectively. The preparation of WPU/GO composites is depicted in Scheme 1.

2.4. Preparation of WPU/GO Films

The WPU/GO films were obtained by casting the WPU/GO nanocomposites onto a Teflon baffle plate, dried at ambient temperature for 7 days, and then at 60 °C in vacuum for 24 h. The films (1 mm) were maintained in a desiccator until future tests.

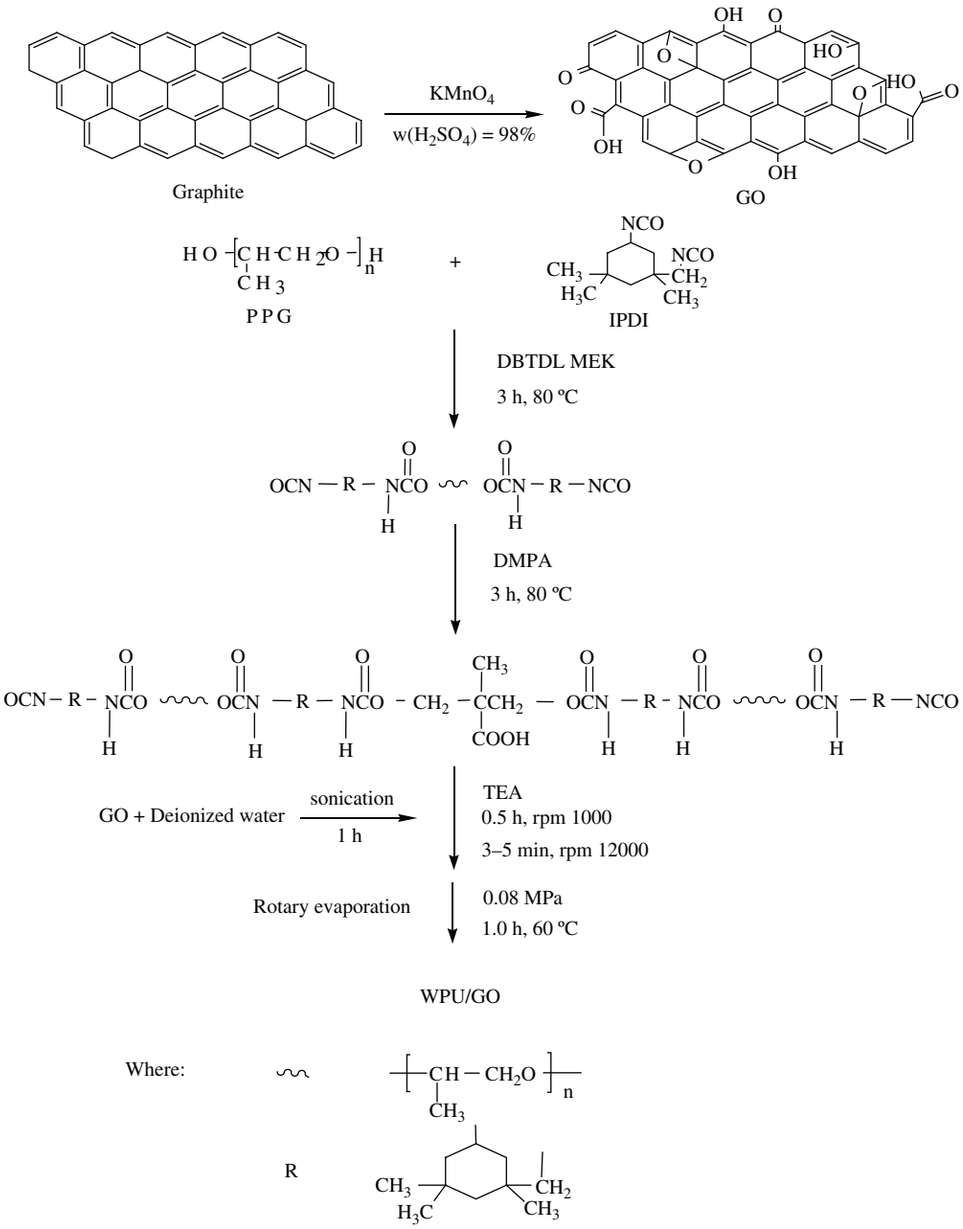

Scheme 1. Synthesis of WPU/GO nanocomposites.

2.5. Characterizations

The stability (zeta potential) and particle size of the WPU/GO emulsions were determined by Horiba SZ 100 series particle size analyzer. The chemical structure of GO and WPU/GO was analyzed with a Nicolet Magna-IR 170 Fourier transform infrared (FT-IR) spectrophotometer. The spectrum was analyzed in the frequency range of 4000–400 cm^{-1}. The crystallinity of GO and WPU/GO films was analyzed by a X-ray diffraction (XRD) on a D8ADVANCE diffractometer (Bruker, Germany) operated at 40 kV and 40 mA. A scanning of 2θ angle was from 5 to 790° at a scanning speed of 0.1 s/step with a scanning step of 0.02°. Scanning electron microscopy (SEM) measurements were performed with an S-4800 (Hitachi) instrument. The samples were prepared by immersing in liquid nitrogen for an hour and breaking quickly. Before SEM examination, the samples were sputter coated with a platinum thin layer for better imaging. Photomicrographs were then taken at an excitation voltage of 15 kV. The GO was characterized by transmission electron microscopy (TEM, Tecnai G20, FEI) after ultrasonicated in de-ionized water for 30 min. The surface hydrophobicity test of the WPU/GO films was carried out on a DCA-315 contact angle measurement apparatus (Beijing Eastern-Dataphy

Instruments Co. Ltd., China) with ultrapure water as probe liquid at room temperature. Water contact angles (WCA) were measured at three different positions for each sample, and the results were expressed as an average value. The surface roughness of the GO and WPU/GO films was observed by multimode atomic force microscopy (AFM, Veeco, USA) in tapping mode at 25 °C and with a scan rate of 1 Hz. Raman spectra of the samples were recorded with a labRAM HR800 (France, Jobin Yvon) using 532 nm laser as the excitation source.

The tensile strength and elongation at break of the WPU/GO dumbbell-shaped tensile samples of 2×20 mm were tested by electric fabric strength tester (YG026T, Changzhou No. 1 Textile Equipment Co. Ltd.) according to Chinese standard GB/T 528-2009 with a pulling speed as 100 mm/min. The data for three measurements were averaged to represent the mechanical properties of the WPU/GO films. The thermogravimetric analysis (TGA) of the WPU/GO films was tested by using a STA449F5 instrument (Netzsch Co. Ltd., Germany). About 5 mg WPU/GO film was tested from 30 to 550 °C with a heating rate of 10 °C/min in nitrogen atmosphere. The thermal property of the WPU/GO films was characterized by using DSC (Q 2000, TA Instruments) in a temperature range of −90–50 °C with a heating rate of 10 °C/min.

3. RESULTS AND DISCUSSION

3.1. The Properties of the WPU/GO Emulsions

The as-prepared WPU/GO emulsions were characterized by a nanoparticle size analyzer. The Zeta potentials presented in Table I confirmed that such aqueous suspensions had good dispersion stability.[26]

As shown in Figure 1, the measured mean size of WPU/GO increased from 60.88 to 105.42 nm with increasing the amount of GO in WPU. The increase in the mean size and broad distribution may be ascribed to the GO nanosheets with one or more layers.

3.2. FT-IR Analysis

Figure 2(a) shows the FT-IR spectra of graphite and GO. A broad absorption band at 3450 cm^{-1} is assigned to the hydroxyl groups on the surface of the GO, the band at 1636 cm^{-1} to the aromatic C═C stretching, and the band at 956 cm^{-1} to the epoxy C–O groups located

Table I. The properties of the WPU/GO emulsions.

Sample	Emulsion appearance	pH	Viscosity/ Pa·s	Zeta potential/mV	Diameter/ nm
WPU0	Milk white	7.83	1.1299	−69.9	60.88
WPU1	Black	7.71	1.2276	−71.3	82.52
WPU2	Black	7.79	1.1750	−70.9	72.52
WPU3	Black	7.65	1.1901	−71.6	105.76
WPU4	Black	7.86	1.2678	−76.6	86.61
WPU5	Black	7.75	1.2343	−75.2	105.42

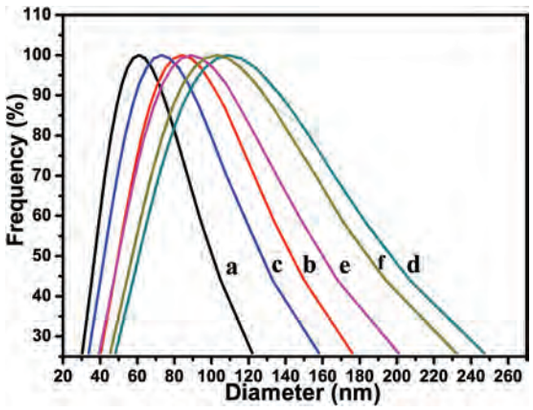

Fig. 1. Particle size distribution for (a) WPU0, (b) WPU1, (c) WPU2, (d) WPU3, (e) WPU4 and (f) WPU5 emulsions.

at the edges of the GO nanosheets.[25] In Figure 2(b), the characteristic absorption peak at about 3340 cm^{-1} is ascribed to the N–H stretching vibration of urethane group, the absorption peaks at 2970 and 2900 cm^{-1} to stretching vibration of C–H and CH_2, the absorption peak at 1716 cm^{-1} to stretching vibration of bonded urethane C═O, while the absorption peak at 1640 cm^{-1} is due to the stretching vibration of bonded urea C═O. These bonded C═O bands indicate the existence of hydrogen

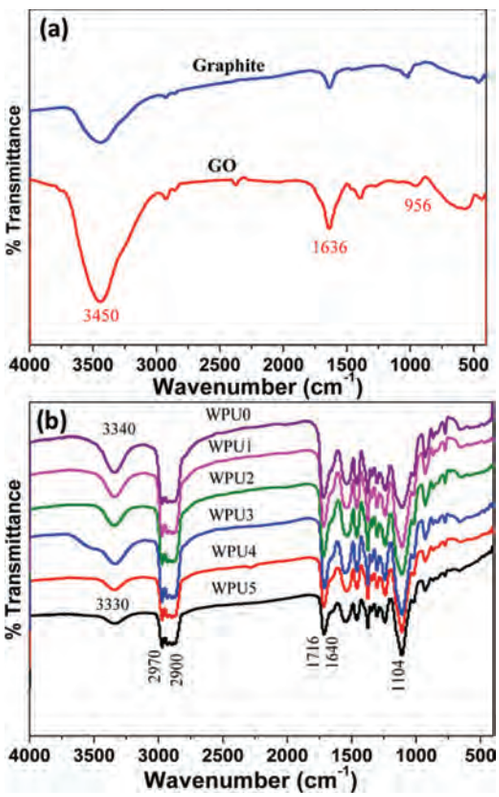

Fig. 2. FT-IR spectra of the (a) graphite and GO, and (b) WPU/GO, respectively.

bonding. The absorption peak at 1104 cm^{-1} is assigned to the stretching vibration of polyether C–O–C. No characteristic peak at 2270 cm^{-1} of free NCO groups observed indicates its complete reaction with OH groups. The FTIR analysis indicates that WPU was successfully synthesized. The position of the –NH peak of WPU0 at 3340 cm^{-1} was shifted to 3333 cm^{-1} in the WPU5 composites due to the covalent interactions and hydrogen bonding between WPU and GO.[20]

3.3. XRD Analysis

Figure 3(a) shows the XRD patterns of graphite and GO. It can be seen that an intense sharp peak at 26.18° is observed and can be assigned to pristine graphite, while the diffraction peak at 11.13° to GO. The *d*-spacing of GO can be calculated according to the Bragg's law(1):[27]

$$2d \sin\theta = n\lambda \quad (1)$$

where λ is the X-ray wavelength, n is the diffraction series and d is the interlayer spacing. The calculated d value of graphite and GO is 0.34 and 0.794 nm, respectively, implying that the sample is expanded when graphite is oxidized. Compared to pristine graphite, the layer-to-layer distance of GO increased obviously. The exfoliation could be caused by the intercalation of oxide functional groups. The weak 2θ peak of the GO indicates the well-exfoliated two-dimensional structures of the GO sheets.

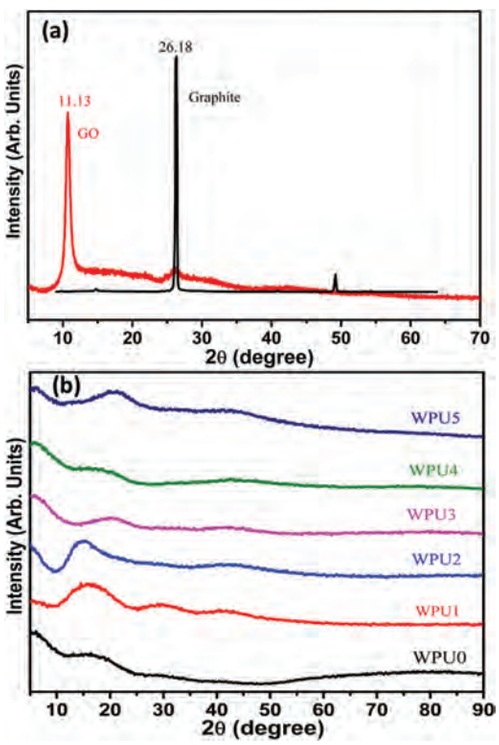

Fig. 3. XRD patterns of the (a) graphite and GO, and (b) WPU/GO, respectively.

The structural features of WPU/GO composites were investigated using XRD in order to detect the presence of intercalated and/or exfoliated microstructures. Figure 3(b) shows the XRD patterns of WPU0, WPU1, WPU2, WPU3, WPU4 and WPU5 composites. Pure WPU0 exhibited a broad characteristics peak at around 16°, corresponding to the crystalline PPG segment in WPU0 and an almost amorphous nature of the cast film.[28] The XRD patterns of WPU1 and WPU2 are similar to that of pure WPU0 and do not display any other crystalline peaks, consistent with the GO nanoparticles being noncrystalline at that size scale. But WPU3, WPU4 and WPU5 have diffraction peaks at about 20.37°, 17.38°, and 21.30°, assigned to the (110) plane and the (200) plane of the PPG crystals, respectively.[29] It means that GO enhanced the crystallization of the PPG segments.[30]

3.4. Morphology of GO and WPU/GO

As shown in Figure 4(a), the pure GO exhibits a folded, smooth surface. In Figure 4(b), the thin layer of GO shows a typical folding nature.[25]

The dispersion state of GO in WPU matrix strongly influences the mechanical property of WPU/GO composite films. Therefore, the dispersion of GO in WPU matrix was investigated by observing the fractured surface morphology using SEM. As shown in Figure 5, the surface of WPU0 was rough and had some fractures. The surfaces of WPU1 and WPU2 films were uneven but dense, and the fracture disappeared. The results indicate that GO and

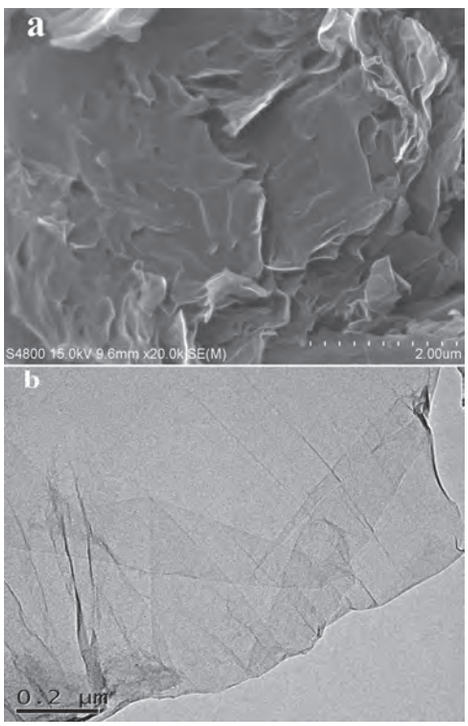

Fig. 4. (a) SEM image of GO; (b) TEM microstructure of GO.

ARTICLE

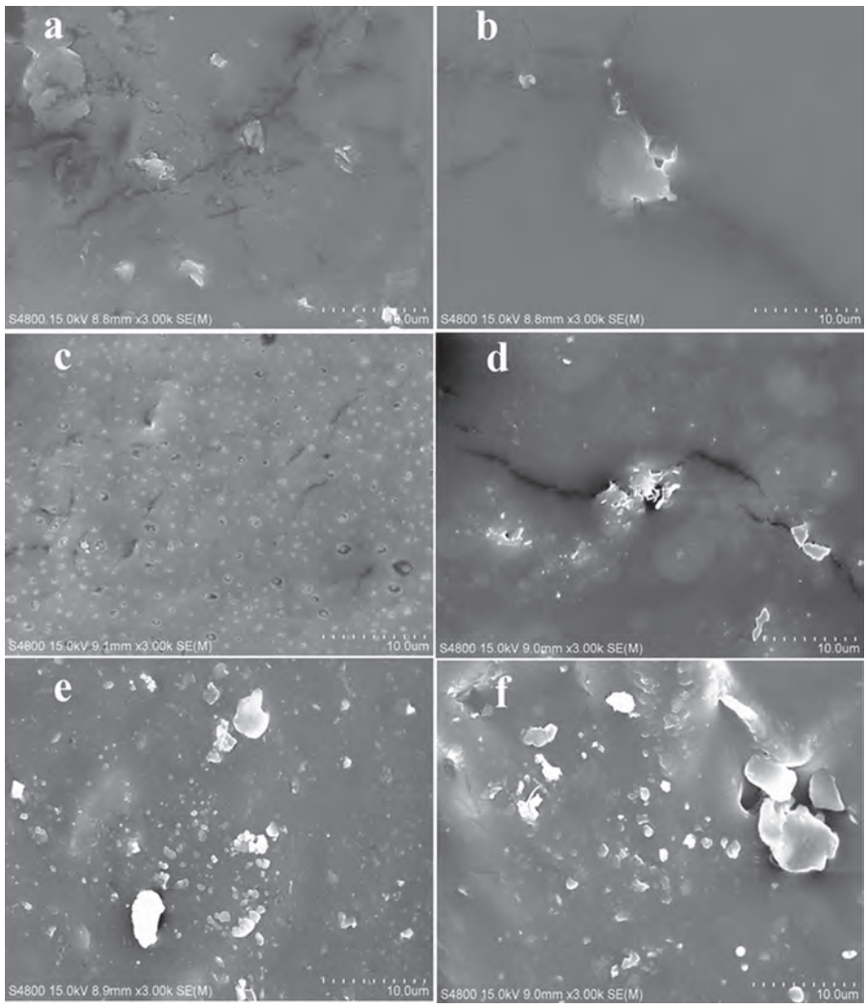

Fig. 5. Fractural surface SEMS for (a) WPU0, (b) WPU1, (c) WPU2, (d) WPU3, (e) WPU4 and (f) WPU5 films.

WPU had a good compatibility beneficial for improving the mechanical properties. The morphologies of WPU3, WPU4, and WPU5 are much more different. There are many irregular projections or aggregations on the fractural surface, resulting from the phase separation. It may be explained by the limited compatibility between GO and WPU. When the amount of GO is too high, the tensile strength decreases with respect to WPU. The SEM result agrees with that of the tensile strength test.[31–33]

Figure 6 displays the AFM image of exfoliated GO sheets with line scan of the selected individual graphene at tapping mode, showing an average roughness (Ra) of 0.224 nm, root mean square roughness (RMS) of 0.478 nm, and maximum height (R_{max}) of 0.997 nm, characteristic of a single layer grapheme.[34]

Figure 7 shows the Raman spectra of GO and natural graphite samples. Raman spectroscopy is a very valuable characterization method for carbon materials. In the Raman spectra of GO and natural graphite samples, the D band originates from the presence of disordered carbon or defects of carbon materials. The G band is usually attributed to the in-plane stretching vibrations of sp^2 hybrid mode carbon atom. As shown in Figure 7, the D and G bands of the samples were located at about 1346–1361 cm^{-1} and 1576–1583 cm^{-1}, respectively. The I_D is the integral area of D band, the I_G is the integral area of G band, while the normalized I_D/I_G ratio is used to measure the amount of disorder of samples. According to calculation, the values of I_D/I_G ratio of GO and natural graphite were 0.876 and 0.090, respectively. The G band is observed to downshift from 1583 to 1576 cm^{-1} due to the recovery of the defects in hexagonal network structure.

The in-plane crystalline size (L_a) is also calculated using an empirical formula Eq. (2):[24,35]

$$L_a = \frac{560}{E_\lambda^4}\left(\frac{I_D}{I_G}\right)^{-1} \quad (2)$$

where E_λ is the excitation laser energy in eV used in the Raman measurement. It is calculated that the La of as-prepared GO is 220 nm.

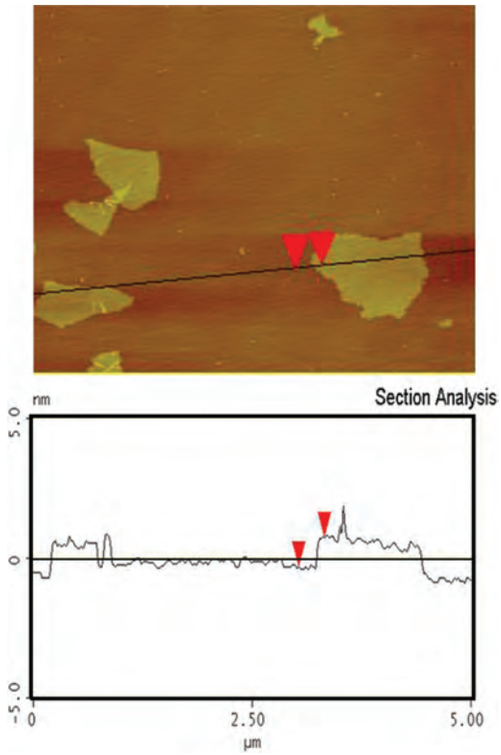

Fig. 6. Tapping mode AFM image of GO.

Figure 8 shows the water contact angles of WPU/GO films. The water contact angle values for the WPU1 and WPU2 films were higher than that of WPU0 and exhibited a slight increase from 58.83° for WPU0 to 61.38° for WPU1 and 62.32° for WPU2, respectively, showing a much better improvement in the hydrophobic properties. This result can be associated with the microstructure forming on the surface of hybrid films caused by the filling of GO. When the added content of the GO was increased to 0.75 wt% and 1.00%, the contact angle values decreased to 58.25 for WPU3, and 55.38 for WPU4. There existed an optimal GO amount around 0.0–0.5% of WPU.

Figure 9 shows AFM images of three dimensional (3D) and surface roughness for WPU0, WPU1, and WPU4

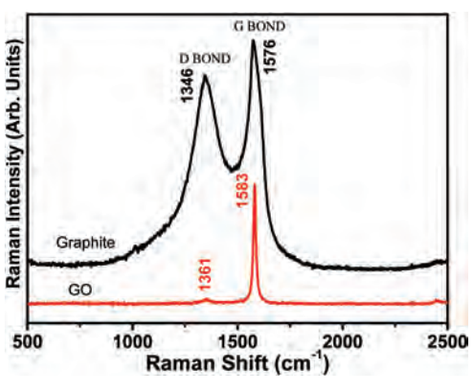

Fig. 7. Raman spectra of graphite and GO.

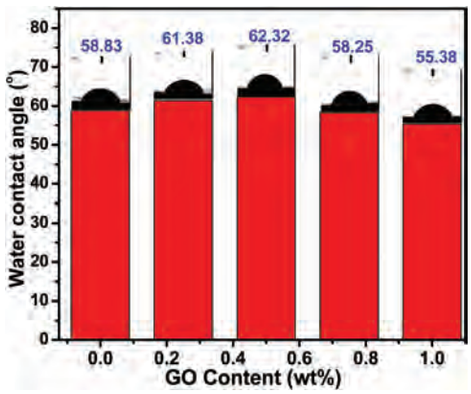

Fig. 8. Water contact angles of WPU/GO films.

films. It is observed that the surface roughness of WPU0, WPU1, and WPU4 films increased with the addition of GO. With increasing the GO content, the black domains of WPU1 decreased and there was no big brighter GO-rich domains in the phase images of WPU1. This is due to the fact that the light part is the dispersion phase composed of hard segments of WPU while the dark part is the continuous phase composed of soft segments of WPU. The surface morphology of WPU1 films exhibits a good compatibility between WPU and GO, which means GO can act as crosslinking points between soft and hard segments, leading to the promotion in the compatibility between the two segments.[36]

3.5. Mechanical Properties

The tensile strength and elongation at break of the WPU/GO films are plotted with bar diagrams in Figure 10. With the GO content increased from 0.00 (WPU0) to 0.25% (WPU1), the tensile strength of the films was improved 60.69%, from 2.90 to 4.66 MPa. Whereas the GO content increased from 0.25 (WPU1) to 0.50% (WPU2), the tensile strength of the films decreased from 4.66 to 4.31 MPa. Hence, the optimal GO content is in the range from 0.25 to 0.50%. With increasing the GO content, the elongation at break of the WPU/GO films decreased correspondingly.

The reduced growth rate can be understood by the special film formation mechanism of the waterborne dispersions, in which the film performance is dominated by the particle coalescence of GO with WPU. The enlarged particle size would have a negative influence on the performance of the film based on the packing of the dispersion particles.[37] This result is correlated to the observation of fractural surface of WPU/GO (Fig. 5).

3.6. Thermogravimetric Analysis

Thermogravimetric and DTG thermograms of WPU/GO are presented in Figure 11. From Figure 11(a), the TGA thermograms of graphite and GO did not lose mass before 500 °C, whereas GO lost a small amount of mass below

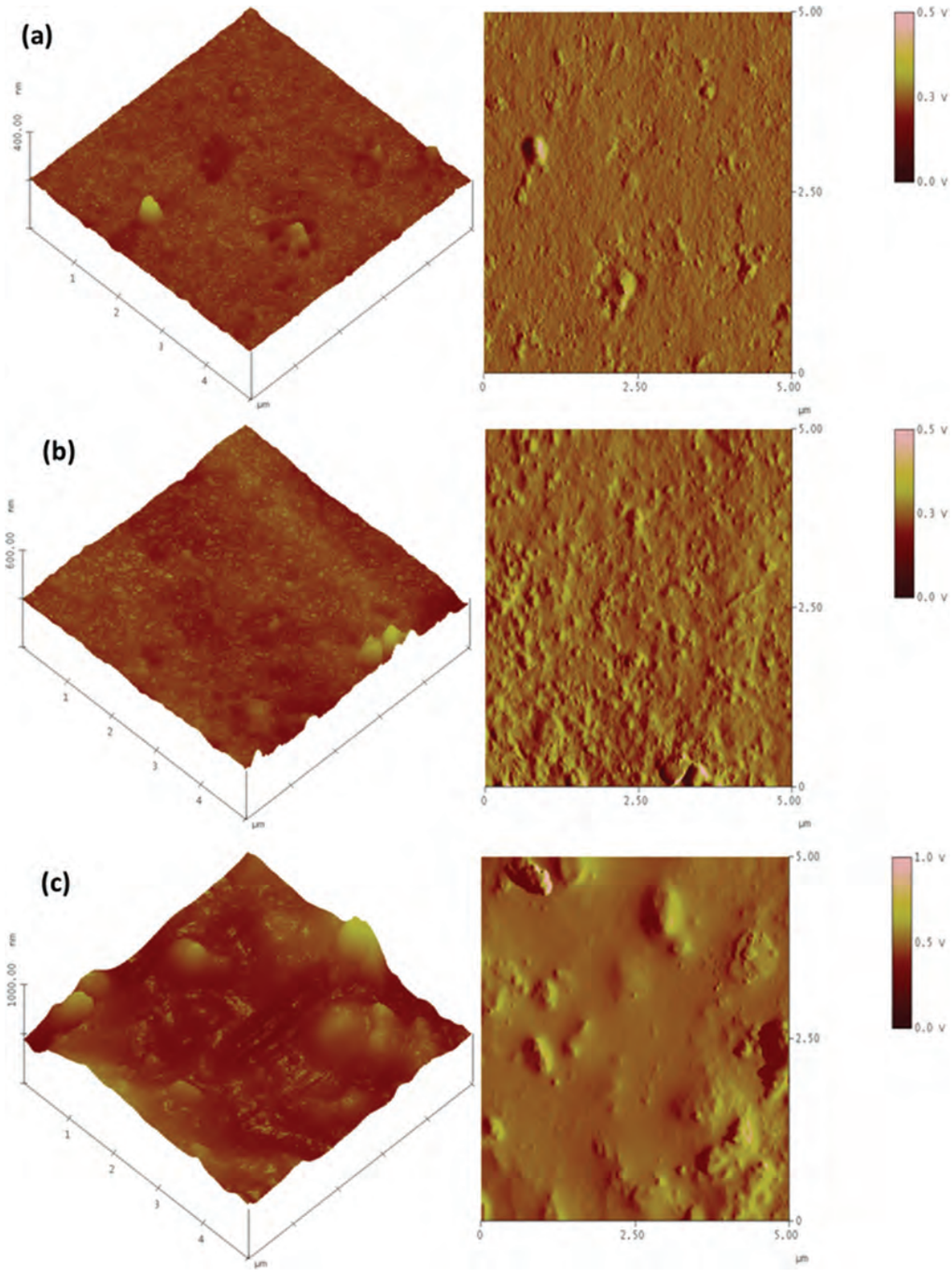

Fig. 9. AFM images of 3D and surface roughness for (a) WPU0, (b) WPU1, and (c) WPU4 films.

100 °C, and underwent a major mass loss (21.02 wt%) at 207.77 °C through the release of CO, CO_2, and water vapor. The decomposition of the oxygen-containing functional groups attached to the carbon plane at 160 °C created a large force between the stacked layers and also reduced the GO.[20] It is clearly indicated from Figure 11(b) that the thermal degradation and stability of WPU0 is related to the hard segment and soft segment structures. The first peak of DTG at 270.37 °C corresponds to the first main decomposition stage of WPU, attributed to the rupture of the urethane bonds. The second peak of DTG at 330.57 °C is attributed to the collapse of urea bonds, and the third peak at 379.70 °C is attributed to the thermal decomposition of soft segments of PPG-2000. The addition of GO had slightly influenced the thermal stability of WPU. It is showed that the hard segment degradation

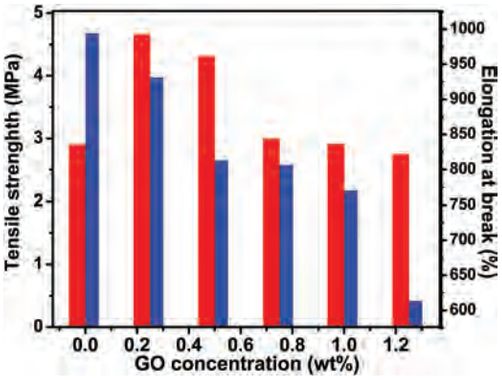

Fig. 10. Bar diagrams of tensile strength and elongation at break of WPU/GO films.

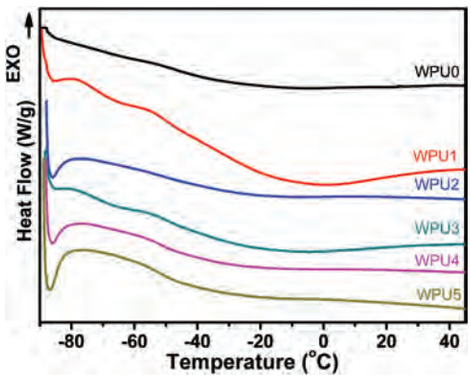

Fig. 12. DSC thermograms of WPU/GO nanocomposites.

of WPU1 and WPU2 was increased, and their soft segment degradation was decreased. Synergistic interactions are expected between WPU and GO due to the reduced microphase separation.[38]

The thermal properties of the WPU/GO nanocomposites were studied by DSC. All of samples show a single glass transition temperature in the range from −52.31 to −29.27 °C, indicating the crystallization for all samples. According to Fang et al.,[39] the glass transition temperatures (T_g) of PPG ($M_n = 2000$) and glycolyzed oligomers are approximately −69 and −43.1 °C, respectively. From Figure 12, it can be seen that the T_g of the WPU1 soft-segments increased from −36.48 to −29.27 °C with 0.25% GO loading. This can be attributed to the good compatibility between the GO and WPU chains and the restricted chain mobility. Yet T_g further decreased at loadings greater than 0.50% (the T_g of WPU2, WPU3, WPU4, and WPU5 were −50.54, −50.01, −51.74, and −52.31 °C, respectively). This decrease may be resulted from the formation of agglomerates in the WPU/GO composites at higher GO loadings.

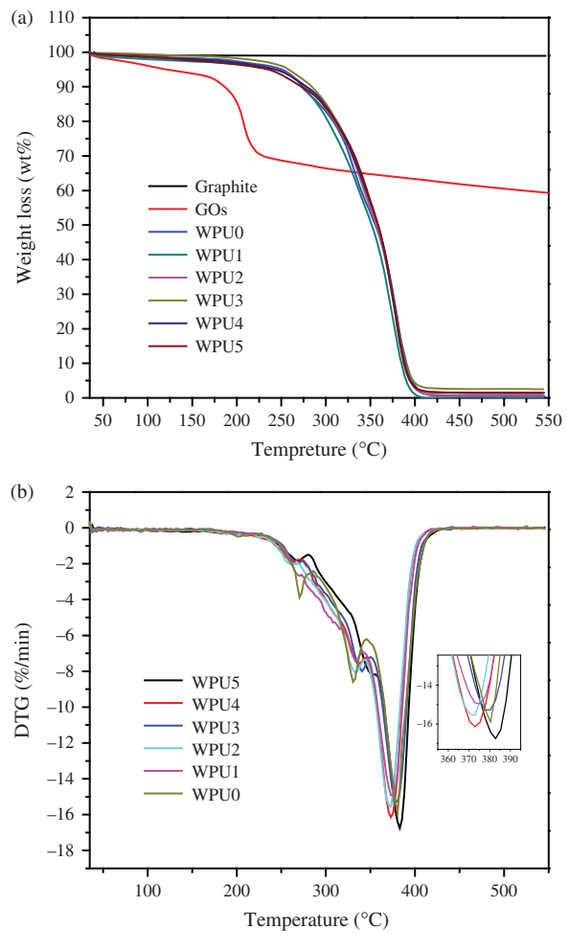

Fig. 11. (a) TG, and (b) DTG curves of GO and WPU/GO nanocomposites.

4. CONCLUSIONS

In this work, a series of WPU/GO composites were prepared by the ultrasonication of GO dispersion and high shear emulsification of WPU pre-polymer. The results showed that the WPU/GO emulsions exhibited good dispersion stability. While the GO amount in WPU/GO nanocomposites was 0.25–0.50 wt% (based on the weight of WPU resin), the GO could be dispersed homogenously. The water contact angle values for the WPU/GO films were higher than that of the pure WPU, which indicated an improved hydrophobic property. Furthermore, when the GO content was increased from 0 to 0.25%, the tensile strength of the films was improved 60.69%. With the increasing GO content, the elongation at break of the WPU/GO films decreased correspondingly. Finally, there were synergistic interactions between WPU and GO because of the reduced micro-phase separation.

Acknowledgment: The authors acknowledge the financial support provided by the State Scholarship Fund of China Scholarship Council (No. 201408410140). This work was also financially supported by 2015 Science and Technology Planning Project of Anyang City, Henan Province, China.

ARTICLE

References and Notes

1. S. L. Cooper and J. Guan (eds.), Advances in Polyurethane Biomaterials, Woodhead Publishing **(2016)**.
2. D. Chattopadhyay and K. Raju, *Progress in Polymer Science* 32, 352 **(2007)**.
3. S. Kumari, A. K. Mishra, D. K. Chattopadhyay, and K. Raju, *Journal of Polymer Science Part A: Polymer Chemistry* 45, 2673 **(2007)**.
4. D. Yang, L. Han, H. Zhang, and F. Qiu, *Journal of Macromolecular Science* Part A 48, 277 **(2011)**.
5. L. Lei, L. Zhong, X. Lin, Y. Li, and Z. Xia, *Chem. Eng. J.* 253, 518 **(2014)**.
6. S. Mirabedini, M. Sabzi, J. Zohuriaan-Mehr, M. Atai, and M. Behzadnasab, *Appl. Surf. Sci.* 257, 4196 **(2011)**.
7. M. Arun, S. Kantheti, R. R. Gaddam, R. Narayan, and K. Raju, *Journal of Polymer Research* 21, 1 **(2014)**.
8. D. Sun, X. Miao, K. Zhang, H. Kim, and Y. Yuan, *J. Colloid Interface Sci.* 361, 483 **(2011)**.
9. L. Wang, Y. Shen, X. Lai, and Z. Li, *J. Appl. Polym. Sci.* 119, 3521 **(2011)**.
10. J. Zhu, S. Wei, N. Haldolaarachchige, D. P. Young, and Z. Guo, *The Journal of Physical Chemistry C* 115, 15304 **(2011)**.
11. S. Zhang, Y. Li, L. Peng, Q. Li, S. Chen, and K. Hou, *Composites Part A: Applied Science and Manufacturing* 55, 94 **(2013)**.
12. J. N. Gavgani, H. Adelnia, and M. M. Gudarzi, *Journal of Materials Science* 49, 243 **(2014)**.
13. M. Hirata, T. Gotou, S. Horiuchi, M. Fujiwara, and M. Ohba, *Carbon* 42, 2929 **(2004)**.
14. Y. R. Lee, A. V. Raghu, H. M. Jeong, and B. K. Kim, *Macromolecular Chemistry and Physics* 210, 1247 **(2009)**.
15. D. A. Dikin, S. Stankovich, E. J. Zimney, R. D. Piner, G. H. Dommett, G. Evmenenko, S. T. Nguyen, and R. S. Ruoff, *Nature* 448, 457 **(2007)**.
16. S. Stankovich, D. A. Dikin, G. H. Dommett, K. M. Kohlhaas, E. J. Zimney, E. A. Stach, R. D. Piner, S. T. Nguyen, and R. S. Ruoff, *Nature* 442, 282 **(2006)**.
17. H. Kim, Y. Miura, and C. W. Macosko, *Chem. Mater.* 22, 3441 **(2010)**.
18. M. J. Allen, V. C. Tung, and R. B. Kaner, *Chem. Rev.* 110, 132 **(2009)**.
19. Y. Zhu, S. Murali, W. Cai, X. Li, J. W. Suk, J. R. Potts, and R. S. Ruoff, *Adv. Mater.* 22, 3906 **(2010)**.
20. P. Pokharel, *Chem. Eng. J.* 253, 356 **(2014)**.
21. Y. Zhuo, J. Liu, Q. Li, B. Qiu, and G. Xing, *Integrated Ferroelectrics* 171, 52 **(2016)**.
22. W. S. Hummers, Jr. and R. E. Offeman, *J. Am. Chem. Soc.* 80, 1339 **(1958)**.
23. L. Lei, Z. Xia, L. Zhang, Y. Zhang, and L. Zhong, *Prog. Org. Coat.* 97, 19 **(2016)**.
24. Y. Wang, Q. He, H. Qu, X. Zhang, J. Guo, J. Zhu, G. Zhao, H. A. Colorado, J. Yu, and L. Sun, *Journal of Materials Chemistry C* 2, 9478 **(2014)**.
25. J. Zhu, M. Chen, H. Qu, X. Zhang, H. Wei, Z. Luo, H. A. Colorado, S. Wei, and Z. Guo, *Polymer* 53, 5953 **(2012)**.
26. N. Liu, Y. Zhao, M. Kang, J. Wang, X. Wang, Y. Feng, N. Yin, and Q. Li, *Prog. Org. Coat.* 82, 46 **(2015)**.
27. W. L. Zhang, B. J. Park, and H. J. Choi, *Chem. Commun.* 46, 5596 **(2010)**.
28. X. Wang, W. Xing, X. Feng, B. Yu, L. Song, G. H. Yeoh, and Y. Hu, *Compos. Sci. Technol.* 127, 142 **(2016)**.
29. J. X. Su, M. B. Zhang, L. Y. Ma, S. P. Zhang, and F. F. Dong, *Advanced Materials Research* 152, 1514 **(2011)**.
30. S. H. Choi, D. H. Kim, A. V. Raghu, K. R. Reddy, H.-I. Lee, K. S. Yoon, H. M. Jeong, and B. K. Kim, *Journal of Macromolecular Science, Part B* 51, 197 **(2012)**.
31. H. Liu, Y. Li, K. Dai, G. Zheng, C. Liu, C. Shen, X. Yan, J. Guo, and Z. Guo, *Journal of Materials Chemistry C* 4, 157 **(2016)**.
32. Y. Xu, W. Hong, H. Bai, C. Li, and G. Shi, *Carbon* 47, 3538 **(2009)**.
33. Y. Lan, H. Liu, X. Cao, S. Zhao, K. Dai, X. Yan, G. Zheng, C. Liu, C. Shen, and Z. Guo, *Polymer* 97, 11 **(2016)**.
34. Y. Geng, S. J. Wang, and J.-K. Kim, *J. Colloid Interface Sci.* 336, 592 **(2009)**.
35. L. Cancado, K. Takai, T. Enoki, M. Endo, Y. Kim, H. Mizusaki, A. Jorio, L. Coelho, R. Magalhaes-Paniago, and M. Pimenta, *Appl. Phys. Lett.* 88, 163106 **(2006)**.
36. M. Iliut, C. Silva, S. Herrick, M. McGlothlin, and A. Vijayaraghavan, *Carbon* 106, 228 **(2016)**.
37. Q. Li, L. Guo, T. Qiu, W. Xiao, D. Du, and X. Li, *Appl. Surf. Sci.* 377, 66 **(2016)**.
38. S. M. Cakić, I. S. Ristić, M. Milena, D. T. Stojiljković, and B. Jaroslava, *Int. J. Adhes. Adhes.* 70, 329 **(2016)**.
39. C. Fang, X. Zhou, Q. Yu, S. Liu, D. Guo, R. Yu, and J. Hu, *Prog. Org. Coat.* 77, 61 **(2014)**.